Liver INTERNATIONAL
OFFICIAL JOURNAL OF THE INTERNATIONAL ASSOCIATION FOR THE STUDY OF THE LIVER

Liver International ISSN 1478-3223

ORIGINAL ARTICLE

Conophylline suppresses hepatic stellate cells and attenuates thioacetamide-induced liver fibrosis in rats

Norio Kubo[1,2], Rie Saito[3], Kunihisa Hamano[3], Masahiro Nagasawa[1], Fumiaki Aoki[1], Izumi Takei[4], Kazuo Umezawa[5], Hiroyuki Kuwano[2] and Itaru Kojima[1]

1 Institute for Molecular and Cellular Regulation, Gunma University, Maebashi, Japan
2 Department of General Surgical Science (Surgery I), Gunma University Graduate School of Medicine, Maebashi, Japan
3 Department of General Medicine, National Defense Medical College, Tokorozawa, Japan
4 Department of Internal Medicine, Tokyo Dental College Ichikawa General Hospital, Ichikawa, Japan
5 Aichi Medical University, Nagakute, Japan

Keywords
apoptosis – collagen – fibrosis – cirrhosis – stellate cell

Correspondence
Itaru Kojima, MD, Institute for Molecular and Cellular Regulation, Gunma University, Maebashi 371-8512, Japan
Tel: +81 27 220 8835
Fax: +81 27 220 8893
e-mail: ikojima@showa.gunma-u.ac.jp

Received 30 January 2013
Accepted 29 August 2013

DOI:10.1111/liv.12328

Abstract

Background & Aims: Conophylline (CnP) is a vinca alkaloid purified from a tropical plant and inhibits activation of pancreatic stellate cells. We investigated the effect of CnP on hepatic stellate cells (HSC) *in vitro*. We also examined whether CnP attenuates hepatic fibrosis *in vivo*. *Method:* We examined the effect of CnP on the expression of α-smooth muscle actin (α-SMA) and collagen-1, DNA synthesis and apoptosis in rat HSC and Lx-2 cells. We also examined the effect of CnP on hepatic fibrosis induced by thioacetamide (TAA). *Results:* In rat HSC and Lx-2 cells, CnP reduced the expression of α-SMA and collagen-1. CnP inhibited DNA synthesis induced by serum. CnP also promoted activation of caspase-3 and induced apoptosis as assessed by DNA ladder formation and TUNEL assay. In contrast, CnP did not induce apoptosis in AML12 cells. We then examined the effect of CnP on TAA-induced cirrhosis. In TAA-treated rats, the surface of the liver was irregular and multiple nodules were observed. Histologically, formation of pseudolobules surrounded by massive fibrous tissues was observed. When CnP was administered together with TAA, the surface of the liver was smooth and liver fibrosis was markedly inhibited. Collagen content was significantly reduced in CnP-treated liver. *Conclusion:* Conophylline suppresses HSC and induces apoptosis *in vitro*. CnP also attenuates formation of the liver fibrosis induced by TAA *in vivo*.

Hepatic stellate cells (HSC) reside in the space of Disse and store vitamin A in lipid droplets under normal conditions (1). Upon liver injury, they are activated and lose lipid droplets. They proliferate actively and differentiate into myofibroblast-like cells (2–4). Chronic liver injuries caused by viral hepatitis, autoimmune hepatitis, alcoholic hepatitis and non-alcoholic steatohepatitis activate and transform quiescent HSC into activated myofibroblasts through the actions of increased growth factors and inflammatory cytokines such as platelet-derived growth factor, transforming growth factor-β (TGF-β), tumour necrosis factor-α (TNF-α), interleukin-6 and IL-1β (4, 5). Activated HSC undergo continuous proliferation and express activation markers such as smooth muscle α-actin (αSMA). They also produce massive extracellular matrix proteins including type I collagen (6). Liver fibrosis is advanced by increasing the production of type I collagen in the extracellular matrix component. Therefore, the majority of antifibrotic therapies are designed to inhibit the activation and proliferation of HSC and to suppress their abilities to produce excess matrix proteins. In this regard, an apoptosis-inducing agent, which selectively induces apoptosis in HSC, would be a potential candidate for antifibrotic treatment (7, 8).

Conophylline (CnP) is a vinca alkaloid extracted from leaves of the tropical plant *Ervatamia microphylla* (9). CnP was shown to mimic the effect of activin A on the differentiation of pancreatic progenitor cells (10). Thus, CnP induces differentiation of pancreatic AR42J cells, a model of pancreatic progenitor cells, into insulin-producing cells and converts cultured ductal cells to β-cells *in vitro* (10, 11). CnP was also effective *in vivo*. This compound promoted differentiation of pancreatic progenitors to β-cells and, when administered to the animal model of diabetes, increased the β-cell mass and the insulin content, and significantly improved hyperglycaemia (12). On the other hand, it is known that activin A is an autocrine activator of pancreatic stellate cells (PSC) and increases the expression of αSMA and collagen (13). This implies that activin A promotes fibrosis of

the pancreas. Interestingly, although CnP reproduces the effect of activin A on β-cell differentiation, this compound has the opposite effect on the activation of PSC. Thus, CnP markedly inhibits the growth of PSC and reduces the expression of αSMA and collagen *in vitro* (14). Furthermore, when administered to an animal model of type 2 diabetes, CnP markedly reduced the invasion of PSC into islets and improved islet fibrosis in GK rats, an animal model of type 2 diabetes (14).

Given the similarity of PSC and HSC, it seems likely that CnP inhibits activation of HSC and thereby attenuates hepatic fibrosis. In this study, we examined the effect of CnP on HSC *in vitro*. We also examined the effect of CnP *in vivo*. The results clearly show that CnP inhibits activation of HSC and improves liver fibrosis induced by thioacetamide (TAA) *in vivo*.

Materials and methods

Materials

Conophylline used in *in vitro* study was isolated from leaves of *E. microphylla* grown in Thailand and purified as described previously (9). Because these leaves are now difficult to obtain, we searched for other sources of CnP and found that leaves of *Tabernaemontana divaricata*, which is grown in a southern island in Japan, also contain CnP (15). Crude CnP preparation II (CCP-II) used in *in vivo* study was obtained from leaves of *T. divaricata*. The method for extraction was described previously (15). CCP-II contained 22 mg/g of CnP. TAA was purchased from WAKO (Osaka, Japan). Nycodenz were obtained from Sigma-Aldrich (St Louis, MO, USA). Collagenase P was from Roche Diagnostics GmbH (Mannheim, Germany). JNK inhibitor II was purchased from Calbiochem (EMD Biosciences Inc., Darmstadt, Germany).

Culture of hepatic stellate cells, hepatocytes and pancreatic ductal cells

Primary HSC were isolated from normal male Wistar rats with body weight of 240–260 g by sequential digestion of the liver with pronase and collagenase, followed by Nycodenz gradient centrifugation as previously described (16). The human immortalized HSC line, Lx-2, was provided by Dr S. L. Friedman of the Mount Sinai Medical School (New York, NY, USA) (17). Both types of cells were cultured in Dulbecco's modified eagle medium (DMEM; WAKO) containing 10% foetal bovine serum (FBS) with penicillin/streptomycin (WAKO), in 5% CO_2 containing humidified atmosphere at 37°C. Primary HSC with two to five passages were used for experiments. Rat hepatocytes were cultured as described previously (18). Pancreatic ductal cells were cultured as described elsewhere (19).

Western blotting

After growing to confluence, HSC were subcultured at equal densities and incubated with DMEM containing 10% FBS. Before the confluence, the medium was changed to serum-free medium and cells were further incubated for 24 h. Pure CnP was dissolved in MeOH and the final concentration of MeOH in culture medium was 0.1%. After 24 h of incubation, cultured HSC were scraped off and collected using a 2× SDS sample buffer [125 mM Tris–HCl (pH 6.8), 4% w/v SDS, and 20% glycerol]. Dithiothreitol at a final concentration of 50 mM was added after the protein assay. Protein concentrations were measured by a commercial kit (BCA™ Protein Assay Kit; PIERCE, Rockford, IL, USA) using BSA as standard. Protein samples (10 μg) were separated by 10% sodium dodecyl sulphate-polyacrylamide gel electrophoresis and transferred to the polyvinylidene fluoride microporous membrane (Immobilon-P; Millipore, Billerica, MA, USA). The membrane was blocked with 5% skim milk in phosphate-buffered saline containing 0.05% Triton X-100 (PBS-T) for 1 h at room temperature, and was then incubated overnight at 4°C with these primary antibodies: anti-αSMA antibody and anti-actin antibody (Sigma-Aldrich) diluted 1:2000, anti-β-tubulin antibody (MP Biomedicals, LLC, Morgan Irvine, CA, USA) diluted 1:2000, anti-JNK antibody, antiphospho-JNK, anti-p38 mitogen-activated protein kinase (MAPK) antibody, antiphospho-p38 MAPK antibody, anti-extracellular signal regulated kinase (ERK) antibody and antiphospho-ERK antibody (Cell Signalling Technology, Danvers, MA, USA) diluted 1: 1000 and anticollagen-1 (Santa Cruz, CA, USA).

After the membranes were washed with PBS-T, they were incubated with a secondary antibody (1:2000) for 1 h at room temperature. The antibody reaction was detected using the enhanced chemiluminescence system (ECL for αSMA, ECL-plus for others; GE Healthcare, Buckinghamshire, UK) and images were obtained by a multipurpose charge-coupled device (CCD) camera system (LAS 4000; Fuji Film Co., Tokyo, Japan). The intensity of the reaction was measured by the analysis software application (Multi Gauge; Fuji Film Co.).

Immunocytochemistry

Hepatic stellate cells were cultured on non-coated glass coverslips at a density of 2×10^4/ml. Cells were fixed with 4% paraformaldehyde for 1 h at room temperature, treated with 50 mM glycine for 6 min, 0.1% (v/v) Triton X-100 in PBS for 5 min, and incubated sequentially with Block Ace® (DS Pharma Biomedical Co, Osaka, Japan). They were incubated with monoclonal mouse anti-αSMA antibody diluted 1:400 for 1 h at room temperature. After washing with PBS, they were incubated with Alexa FluorR 488 goat antimouse IgG (H + L) conjugate (1:2000) (Invitrogen, Carlsbad, CA, USA) for 1 h and then 4′diamino-2-phenylindole (DAPI: PIERCE,

Rockford, IL, USA). Immunofluorescence images were recorded with an Olympus AX70 Epifluorescence microscope (Olympus, Tokyo, Japan) equipped with a PXL 1400 cooled-CCD camera system (Photometrics, Tucson, AZ, USA), which was operated with IP Lab Spectrum software (Signal Analysis, Vienna, VA, USA).

Measurement of collagen

Collagen was determined by a dye-binding method (Sircol collagen assay; Biocolour Ltd, Carrickfergus, UK). The Sirius red dye reagent binds specifically to the $(Gly\text{-}X\text{-}Y)_n$ helical structure found in all collagen types. After 24 h of serum starvation, HSC were incubated in the presence of CnP and 10 ng/ml TGF-β in medium containing 10% FBS for 48 h. Assay of each culture was performed according to the manufacturer's instructions. In short, 1 ml of Sirius red dye reagent was added to each sample and mixed by shaking for 30 min to complete collagen-dye binding. After centrifugation at 10 000*g* for 10 min, unbound dye was decanted. The dye bound to the collagen pellet was then dissolved in 1 ml of alkali reagent. The dye concentration was measured by spectrophotometry at 550 nm. Hydroxyproline was measured according to the method by Reddy and Enwemeka (20).

Measurement of macrophage chemoattractant protein-1

Hepatic stellate cells were incubated in the same condition for assay of collagen secretion. Macrophage chemoattractant protein-1 (MCP-1) in the culture medium was measured by ELISA (Therm Fisher Scientific, Rockford, IL, USA).

Detection of apoptosis

TUNEL assay. For the TUNEL assay, HSC plated on coverslips were washed with ice-cold PBS three times for 5 min, fixed with 4% paraformaldehyde for 25 min and washed three times with PBS. The coverslips were washed with 0.2% PBS-T for 15 min. TUNEL assay was performed using a fluorescent DNA fragmentation detection kit (Promega, Madison, WI, USA) according to the manufacturer's instructions. The field was chosen randomly and 10 fields were chosen for every specimen. The number of TUNEL-positive cells was counted to obtain the ratio of TUNEL positivity to the total number of cells stained with DAPI.

Measurement of DNA fragmentation

Hepatic stellate cells were incubated for 48 h in DMEM containing 10% FBS. The medium was then changed to DMEM without FBS, and the cells were incubated with CnP for 24 h. The cells were washed with ice-cold PBS and scraped with 250 μl of ice-cold PBS and 250 μl of lysis buffer (50 mM Tris/HCl (pH 8.1), 20 mM ethylenediamine tetraacetic acid (EDTA) (TE) and 0.5% Triton X-100). Lysed cells were held at 4°C for 15 min, and centrifuged at 9000*g* for 10 min. The supernatants were mixed with 0.5 ml of TE-saturated phenol and centrifuged at 13 000*g* for 10 min. The supernatants were mixed with 0.5 ml of chloroform and centrifuged at 13 000*g* for 5 min. The supernatants were mixed with 40 μl of 3 M Na acetate and 800 μl of 100% ethanol, incubated overnight at −20°C and centrifuged at 20 000*g* for 10 min.

To perform the DNA fragmentation assay, the DNA pellet was dissolved in 15 μl of TE buffer (10 mM Tris–HCl (pH 8.1), and 1 mM EDTA) together with 1 μl of RNase A (20 mg/ml) and incubated at 37°C for 1 h. Electrophoresis was run at 100 V in 2% agarose gels in 0.5 × TBE buffer (44.5 mM Tris, 44.5 mM boric acid, 1 mM EDTA). The gel was incubated in ethidium bromide for 10 min. The DNA fragmentation pattern was visualized with a UV transilluminator.

Measurement of caspase-3 activation

Fluorescence resonance energy transfer images were captured using an inverted microscope (IX-81, Olympus) equipped with a cooled 3CCD camera (ORCA-3CCD, Hamamatsu Photonics, Hamamatsu, Japan). The excitation light source was provided by a 150W Xenon lamp (Olympus) and was used for simultaneous capturing images of ECFP and Venous. The cells expressing SCAT 3.1 were incubated in Hank's balanced salt solution containing 0.5 μg/ml CnP (21). Live cell images were acquired at a rate of 60 s.

Assessment of apoptotic bleb

PM-EYFP plasmid was purchased from Clonthech (Mountain View, CA, USA). HSC cells transduced with PM-EYFP, which was used as a plasma membrane marker (22), were incubated with 0.5 μg/ml CnP. Live cell images were acquired at a rate of 60 s.

Measurement of DNA synthesis

DNA synthesis was assessed by measuring [^{3}H]thymidine incorporation. After the incubation in serum-free medium for 48 h, cells were cultured in various conditions for 48 h and 0.5 mCi/ml [^{3}H] thymidine was included in the last 4 h. After incubation, cells were washed twice with ice-cold PBS, solubilized and radioactivity associated with trichloroacetic acid-precipitable materials was counted.

Animals and induction of cirrhosis by thioacetamide

All animal experiments were performed with the permission of the Animal Care and Experimentation Committee, Gunma University. Sprague-Dawley rats with a mean body weight of 70–80 g were purchased from Charles River Japan (Yokohama, Japan). Rats were

maintained in a climate-controlled (21°C) room under 12 h light–dark cycles and were given tap water and standard laboratory chow. Cirrhosis was induced by intraperitoneal injections of TAA (200 mg/kg body weight), administered three times a week for a period of 12 weeks (23). The body weight was measured every week. The animals were sacrificed 5 days after the last treatment, the body weight and liver weight were measured and photos were taken. Formalin-fixed liver tissue was embedded in paraffin, and sections were stained with haematoxylin and eosin and Masson's staining.

Treatment with conophylline (CCP-II)

Rats were randomly divided into three groups. All rats were given TAA for 12 weeks. In the CnP group, 0.9 μg/g of CnP were administered via an oral tube every day for 12 weeks, and in the control group, vehicle was administered via an oral cannula. In the *in vivo* study, CCP-II was used. CCP-II was diluted in 4.09 mg/ml of water containing 0.5% Tween-80 solution.

The serum CnP concentration peeked at 3 h after the oral administration and then decreased gradually to 6% of the peak value by 24 h (15).

Quantitative analysis of fibrosis in the liver

Quantification of the collagen content was performed in formalin-fixed, paraffin-embedded tissue sections after the Masson's trichrome staining. Masson's trichrome-positive areas were measured using the Image J 1.44 image analysis software (National Institute of Health, Bethesda, MA, USA) by means of a CX41 microscope (Olympus) with a DP21 digital camera (Olympus). The amount of collagen deposition was calculated from 25 randomized and non-overlapping areas at ×20 magnification.

Statistical analysis

Results were expressed as means ± SD. For comparison between the two groups, the unpaired *t*-test was used. $P < 0.05$ was considered to be significant.

Results

Effect of conophylline on hepatic stellate cells

We first examined whether or not CnP affected HSC *in vitro*. Rat HSC in primary culture were incubated with various concentrations of CnP in medium containing 5% FBS for 48 h. In the absence of CnP, HSC extended the process and stress fibre-like structure was clearly observed. The stress fibre-like structure was reduced by CnP in a dose-dependent manner. Also, the size of the cells was reduced by CnP (Fig. 1A). At a concentration of 100 ng/ml, CnP markedly reduced the immunoreactivity of αSMA. Similar effects were observed with Lx-2 cells, a cell line of HSC (data not shown). Subsequent studies were done in Lx-2 cells. We then measured changes in the expression of αSMA and collagen-1 by immunoblotting. CnP suppressed the expression of αSMA in a dose-dependent manner. Likewise, the expression of collagen-1 was reduced by CnP in a dose-dependent manner (Fig. 1B–D). CnP at a concentration of 100 ng/ml markedly reduced the expression of both αSMA and type 1 collagen. Consistent with these results, collagen secreted to the medium was also reduced significantly by CnP (Fig. 1E). CnP also inhibited secretion of MCP-1 in a dose-dependent manner (Fig. 1F).

We next examined the effect of CnP on DNA synthesis by measuring [^{3}H]thymidine incorporation in Lx-2 cells. As shown in Figure 2A, thymidine incorporation induced by 5% serum was markedly decreased by CnP in a dose-dependent manner. At a concentration of 100 ng/ml, CnP inhibited [^{3}H]thymidine incorporation by 20%. At this concentration, CnP did not affect [^{3}H]thymidine incorporation in AML12 cells, a cell line resembling mature hepatocytes.

Likewise, 100 ng/ml CnP did not inhibit DNA synthesis in rat hepatocytes in primary culture (Fig. 2B). Furthermore, CnP did not affect DNA synthesis at the same concentration in rat pancreatic ductal cells (Fig. 2C).

Induction of apoptosis by conophylline

We next examined whether or not CnP induced apoptosis in HSC using Lx-2 cells. Lx-2 cells were cultured on coverglass for 12 h with various concentrations of CnP. The number of TUNEL-positive cells was significantly increased in CnP-treated cells (Fig. 3A). The effect of CnP was dose-dependent and at 100 ng/ml approximately 10% of the cells were TUNEL-positive (Fig. 3B). In this condition, DNA fragmentation was observed in CnP-treated cells (Fig. 3C). Next, we monitored caspase-3 activation in Lx-2 cells using cells transfected with SCAT3.1. The colour in the Lx-2 cells was turned from blue (a) to red (d) several minutes after the administration of 100 ng/ml CnP, indicating that caspase-3 was activated in these cells (Fig. 3D). Lx-2 cells were then transfected with PM-EYFP in order to observe morphological changes in the plasma membrane. Apoptotic bleb in the plasma membrane was observed several minutes after the administration of CnP and the cell was contracted after the CnP treatment (Fig. 3E). Note that CnP did not activate caspase-3 in AML12 hepatocytes (Fig. 3F). We then measured changes in the expression of proteins involved in induction of apoptosis by immunoblotting. CnP did not affect the expression of Bcl-2, Bax or procaspase-9. As shown in Figure 4, CnP increased the protein level of cleaved caspase-3.

Effect of conophylline on mitogen-activated protein kinase signalling pathways

We previously showed that CnP induces differentiation of pancreatic β-cells by activating p38 mitogen-activated

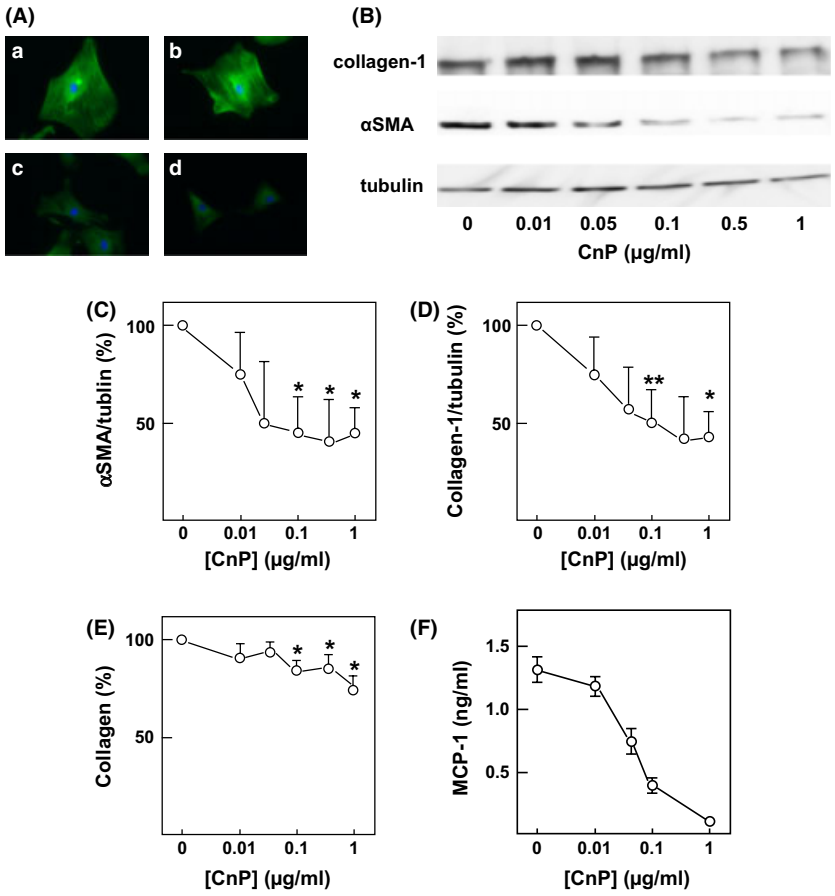

Fig. 1. Effect of CnP on cultured HSC. (A) Effect of CnP on the expression of αSMA in HSC. Rat cultured HSC were incubated for 24 h with various concentrations of CnP and then immunostained with anti-αSMA antibody. a: none, b: 0.01 μg/ml CnP, c: 0.1 μg/ml CnP, d: 1 μg/ml CnP. (B) Effect of CnP on the expression of collagen-1 and αSMA. Lx-2 cells were incubated for 24 h with various concentrations of CnP and the expression of collagen-1 and αSMA was determined by immunoblotting. (C) Quantification of the effect of CnP on the expression of αSMA. Expression of αSMA shown in (B) was quantified by densitometry. Values are the mean ± SD ($n = 4$). *$P < 0.05$ vs without CnP. (D) Quantification of the effect of CnP on the expression of collagen-1. Expression of collagen-1 shown in (B) was quantified by densitometry. Values are the mean ± SD ($n = 4$). *$P < 0.05$ vs without CnP, **$P < 0.01$ vs without CnP. (E) Effect of CnP on secretion of collagen. Lx-2 cells were incubated for 48 h with 10 ng/ml TGF-β and various concentrations of CnP. Collagen secreted to the culture medium was measured. Values are the mean ± SD ($n = 4$). *$P < 0.05$ vs without CnP. (F) Effect of CnP on secretion of MCP-1. Lx-2 cells were incubated for 48 h with 10 ng/ml TGF-β and various concentrations of CnP. MCP-1 secreted to the medium was measured. Values are the mean ± SD ($n = 4$).

kinase (MAPK) (10, 11). We therefore examined whether or not CnP activated MAPKs in HSC. Lx-2 cells were incubated with DMEM containing 100 ng/ml CnP for various periods and activation of MAPKs was measured. As shown in Figure 5A, CnP markedly increased phospho-JNK. The effect of CnP was rapid and transient. Increase in phospho-JNK was detected within 15 min and returned to the basal levels by 60 min. Other types of MAPKs including Erk and p38 were also affected by CnP but the effect of CnP was not as great as that on JNK. We then examined whether or not apoptosis-inducing activity of CnP was mediated by JNK. To this end, we used JNK inhibitor II. Lx-2 cells were pretreated with 20 μM JNK inhibitor II and CnP was then administered. As shown in Figure 5B, JNK inhibitor II did not affect the number of TUNEL-positive cells induced by CnP. Also, JNK inhibitor II did not inhibit formation of DNA ladder induced by CnP (Fig. 5C). Likewise, PD098059 and SB203580, inhibitors of Erk and p38, respectively, did not influence the effect of CnP (data not shown).

Effect of conophylline on liver fibrosis in thioacetamide-treated rats

To induce hepatic fibrosis, TAA was injected intraperitoneally three times a week and CnP was orally administered every day. Twelve weeks later, the body weight of control and CnP-treated rats was not changed (Table 1).

The morphology of the liver in rats after the administration of TAA was very different in control and

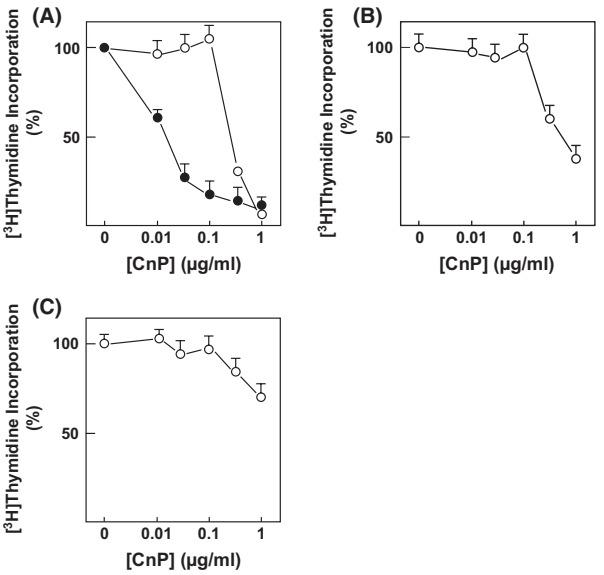

Fig. 2. Effect of CnP on DNA Synthesis in Lx-2 and AML12 Cells. (A) Lx-2 cells (●) and AML12 cells (○) were incubated for 48 h with various concentrations of CnP and [^{3}H]thymidine incorporation was measured as described in Methods. Values are the mean ± SD (n = 4). (B) Rat hepatocytes were incubated for 48 h with 10% serum and various concentrations of CnP and [^{3}H]thymidine incorporation was measured. Values are the mean ± SD (n = 4). (C) Rat pancreatic ductal cells were incubated for 48 h with 10% serum and various concentrations of CnP and [^{3}H]thymidine incorporation was measured. Values are the mean ± SD (n = 4).

CnP-treated groups. Macroscopically, the surface of the liver was irregular and a high number of nodules were observed in the livers of the control group (Fig. 6A-a). In contrast, the surface of the liver was smooth and nodules were not observed in the CnP-treated groups (Fig. 6A-b). In control group, some rats had ascites at the time of sacrifice. Histologically, the sinusoidal structure was completely destroyed and the formation of cirrhotic nodules was observed in control rats (Fig. 6A-c). In contrast, sinusoidal structure was maintained and no nodules were found in the specimen of CnP-treated rats (Fig. 6A-d). By Masson's trichrome staining, an increased fibrotic area with typical bridging fibrosis was observed in control rats (Fig. 6A-e). In CnP-treated rats, however, cirrhotic nodules were rarely observed and fibrosis was minimal (Fig. 6A-f). When the liver specimens were immunostained with the anti-αSMA antibody, numerous αSMA-positive cells were found in the perifibrotic area in control rats (Fig. 6B-a, B-c). In contrast, αSMA-positive cells were found only in the perivascular area in CnP-treated rats (Fig. 6B-d). The fibrotic area was quantified in slices stained with Masson's trichrome by using Image J. The fibrotic area was significantly decreased in CnP-treated group than in the control group (Fig. 7A).

Collagen content was then measured using liver tissue from control and CnP-treated rats by the Sircol collagen assay. The collagen content in CnP-treated group was significantly decreased compared to that of the control group (Fig. 7B). Collagen content in the liver measured by immunoblotting was also reduced in CnP-treated rats (Fig. 7C, D). Similarly, CnP significantly reduced the hydroxyproline content (Fig. 7E).

We also examined whether or not CnP was effective in reversing established hepatic fibrosis. To this end, we administered TAA for 12 weeks. Either CnP or vehicle was then administered for 4 weeks. Rats were then sacrificed and liver samples were obtained. Macroscopically, there was no apparent difference in the two groups. Microscopically, liver fibrosis was slightly improved in both groups compared to that in rats treated with TAA for 12 weeks but there was no morphological difference between vehicle- and CnP-treated rats (data not shown).

Discussion

Hepatic stellate cells are key cellular components involved in the development of hepatic fibrosis. When exposed to soluble factors, including reactive oxidative radicals, growth factors or cytokines released from damaged hepatocytes, activated Kupffer cells, endothelial cells, infiltrating macrophages and neutrophils, HSC undergo morphological transition to myofibroblast-like cells (1, 24, 25). Activated HSC produce massive extracellular matrix proteins and also further promote inflammation by secreting chemokines. Hence, activation of HSC is a central event in the pathogenesis of liver fibrosis and cirrhosis (26). Consequently, HSC are a major target for the treatment of liver fibrosis.

In this study, we assessed suppressive effects of CnP on HSC both *in vitro* and *in vivo*. Quiescent HSC undergo spontaneous activation when plated on uncoated plastic dishes. They obtain a myofibroblast-like phenotype accompanied by loss of vitamin A and increased expression of αSMA and type 1 collagen (26, 27). As shown in Figure 1, CnP decreased the expression of αSMA and type 1 collagen in a dose-dependent manner and significantly reduced secretion of collagen into the medium. These results are in good agreement with the previous results obtained in PSC (14).

Conophylline also inhibited DNA synthesis in HSC as assessed by [^{3}H]thymidine incorporation. Interestingly, the suppressive effect of CnP on DNA synthesis was dependent on the cell type. Thus, while 0.1 μg/ml CnP nearly completely suppressed DNA synthesis in HSC, this compound was essentially without effect in AML12 hepatocytes, rat hepatocytes in primary culture and pancreatic ductal cells in primary culture (Fig. 2). Furthermore, CnP induced apoptosis of HSC: CnP activated caspase-3, induced apoptotic blebs in the plasma membrane and caused ladder formation of DNA. Again, the apoptosis-inducing effect of CnP was dependent on the cell type and CnP did not activate caspase-3 in AML12 hepatocytes. CnP also inhibits secretion of

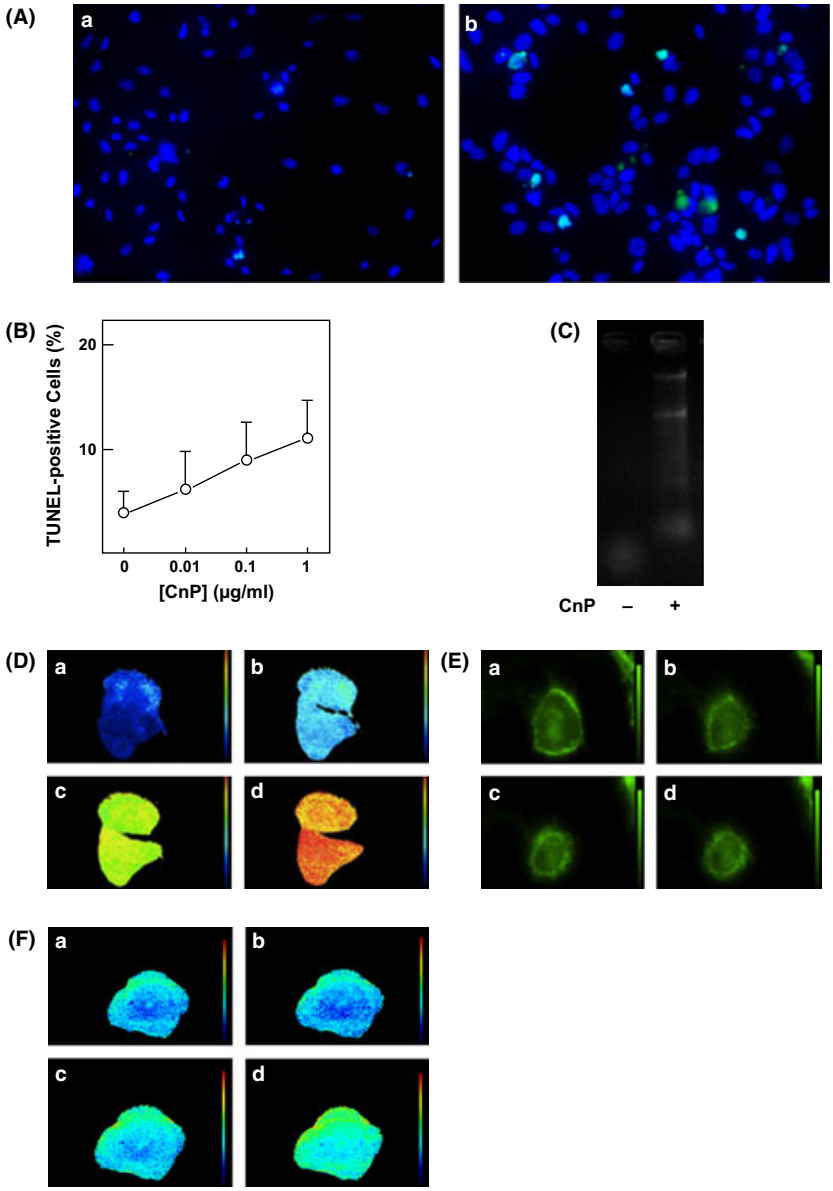

Fig. 3. Effect of CnP on apoptosis in Lx-2 Cells. (A) Lx-2 cells were incubated for 24 h in serum-free medium with (b) or without (a) 0.1 μg/ml CnP. TUNEL staining was done as mentioned in Methods. (B) Lx-2 cells were incubated for 24 h in serum-free medium containing various concentrations of CnP. The number of TUNEL-positive cells was counted. Values are the mean ± SD (n = 4). (C) Effect of CnP on DNA Ladder Formation. Lx-2 cells were incubated for 12 h in the presence and absence of 0.1 μg/ml CnP and DNA ladder formation was determined. The result is a representative of five experiments. (D) Effect of CnP on activation of caspase-3 in Lx-2 Cells. Lx-2 cells expressing SCAT3.1 were incubated with 0.1 μg/ml CnP and FLET images were obtained at 0 (a), 2 (b), 5 (c) and 10 (d) min. Warm colour indicates the activation of caspase-3. The figure shows changes in the fluorescence in typical two cells and the results are representative of three experiments. (E) Effect of CnP on the formation of apoptotic bleb in Lx-2 cells. Lx-2 cells expressing PM-YFP were incubated with 0.1 μg/ml CnP and YFP signal was detected at 0 (a), 2 (b), 5 (c) and 10 (d) min. The plasma membrane is visualized in green. The figure shows changes in the fluorescence in a typical cell and the results are representative of four experiments. (F) Effect of CnP on activation of caspase-3 in AML12 cells. AML12 cells expressing SCAT3.1 were incubated with 0.1 μg/ml CnP and FLET images were obtained at 0 (a), 2 (b), 5 (c) and 10 (d) min. Warm colour indicates the activation of caspase-3. Compare this figure with (D). The figure shows changes in the fluorescence in a typical cell and the results are representative of three experiments.

MCP-1 from HSC (Fig. 1F). CnP perhaps inhibits recruitment of macrophages and suppresses innate immunity to some extent. CnP is a vinca alkaloid purified from a tropical plant. Originally, CnP was isolated as a compound that reversed the morphological changes induced by K-*ras*. Subsequently, CnP was shown to induce differentiation of pancreatic progenitor cells to β-cells (10, 11, 28). The effect of CnP was independent

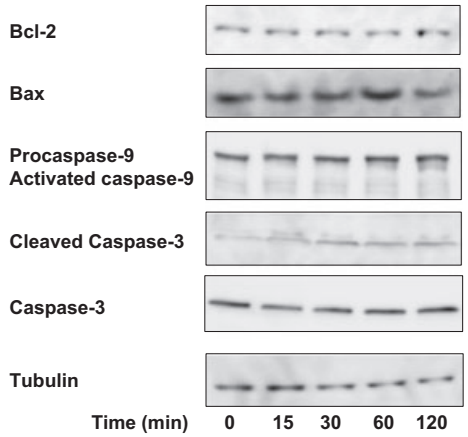

Fig. 4. Effect of CnP on the expression of Bcl-2, Bax, caspase-9 and caspase-3. Lx-2 cells were incubated for various periods of time and the expression of Bcl-2, Bax, activated caspase-9 and cleaved caspase-3 was measured by immunoblotting. The results are representative of four experiments.

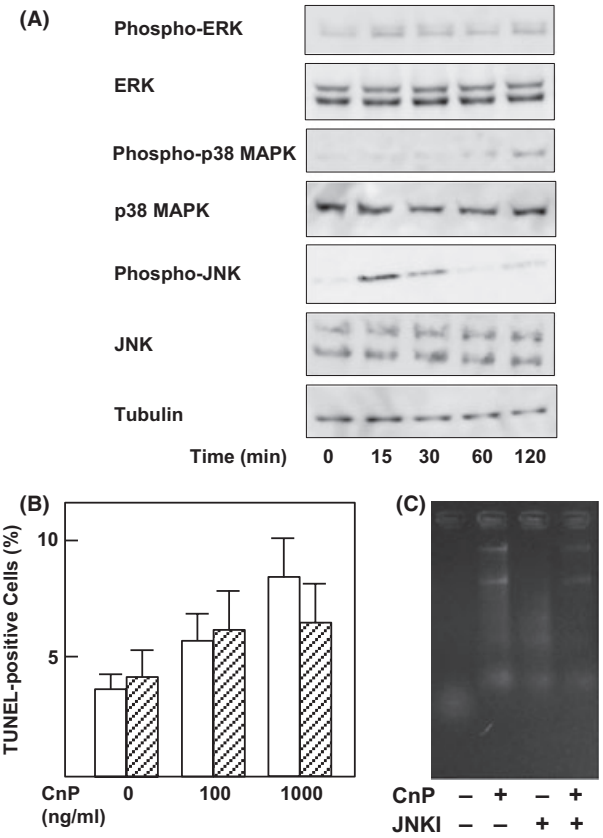

Fig. 5. Effect of CnP on activation of MAP kinases. (A) Lx-2 cells were incubated with 0.1 μg/ml CnP for various periods of time and activation of ERK, p38 and JNK was measured by immunoblotting. The results are representative of three experiments. (B) Effect of JNK inhibitor II on CnP-induced apoptosis. Lx-2 cells were incubated with 0.1 μg/ml CnP for 24 h in the presence (shaded column) and absence (open column) of JNK inhibitor II and the number of TUNEL-positive cells was counted. Values are the mean ± SD (n = 4). (C) Effect of JNK inhibitor II on CnP-induced DNA ladder formation. Lx-2 cells were incubated for 12 h with or without 0.1 μg/ml CnP in the presence and absence of JNK inhibitor II (JNKI). DNA ladder formation was measured. The results are representative of six experiments.

of Ras. In fact, CnP induced differentiation by up-regulating the expression of neurogenin-3, a critical transcription factor involved in differentiation of pancreatic endocrine cells (11). This effect of CnP was mediated by p38 MAPK. Thus, CnP stimulates the expression of neurogenin-3 by activating p38 MAPK (11). As shown in Figure 5, CnP activated three types MAPKs – Erk, JNK and p38 – in HSC. Nevertheless, inhibition of these MAPKs did not alter the effect of CnP on HSC. In general, activation of MAPKs is thought to activate HSC (2–4). However, CnP effectively blocked activation of HSC. This implies that CnP may generate a strong signal(s) to suppress HSC. At present, we have not identified the mechanism of action of CnP in HSC. Further studies are clearly needed to identify the site and mechanism of action of CnP in HSC.

We assessed the *in vivo* effect of CnP using TAA-induced cirrhosis model in rats. The doses of CnP (0.9 μg/g) used in *in vivo* and *in vitro* experiments were the same as those used in our previous study in the pancreas (14, 15), which demonstrated no apparent side effects. In particular, CnP did not induce haematological dysfunction (15). In agreement with this, side effects were not observed in this study. In our *in vivo* study, we used CCP-II, partially purified preparation of CnP. As mentioned previously, purified CnP and CCP-II had essentially the same effects *in vitro* (14). A major contaminant in CCP-II is a conophillidine (15), which has a CnP-like structure with CnP-like action. Accordingly, CCP-II is slightly more potent than expected in terms of suppressing stellate cells (14). Collectively, it seems likely that suppression of HSC by CCP-II *in vivo* is caused by CnP rather than contaminant in CCP-II preparation. We showed that CnP markedly reduced the fibrosis in the rat liver. Previous reports showed that liver fibrosis induced by CCl_4 or TAA was suppressed by armepavine (29), follistatin (30), salvianolic acids (31) and other agents (32–37). Compared to these compounds, suppression of liver fibrosis by CnP was much more significant; indeed, the effect of CnP was visible on the surface of the liver. Microscopically, the suppressive effect of CnP was observed in the H.E. stained specimen. Thus, cirrhotic nodules typical of cirrhosis were absent in CnP-treated rats and histological architecture of sinusoid was maintained. Because of Masson's trichrome staining, massive fibrous tissues surrounding pseudolobes were almost absent in CnP-treated rats. Furthermore, invasion of αSMA-positive HSC surrounding pseudolobes was not observed in CnP-treated rats. Taken together, morphological

Table 1. Effect of CnP on various parameters in TAA-treated rats

	BW (g)	LW (g)	Albumin (mg/dl)	AST	ALT	T-bil	Glucose
Control	309.6 ± 37.5	16.5 ± 2.8	0.88 ± 0.15	88.3 ± 28.6	46.3 ± 11.4	0.12 ± 0.04	120 ± 16
CnP	294.2 ± 50.2	14.4 ± 3.5*	0.99 ± 0.13	103.9 ± 79.1	42.9 ± 18.0	0.17 ± 0.21	133 ± 17

Rats were treated with TAA for 12 weeks and CnP (0.9 or 1.8 μg/g) or vehicle was administered. Five days after the last administration of TAA, rats were sacrificed and the body weight, liver weight, albumin, aspartate aminotransferase (AST), alanine aminotransferase (ALT), total bilirubin (T-bil) and plasma glucose concentration (glucose) were measured. Values are the mean ± SD (n = 9). *P < 0.05 vs control.

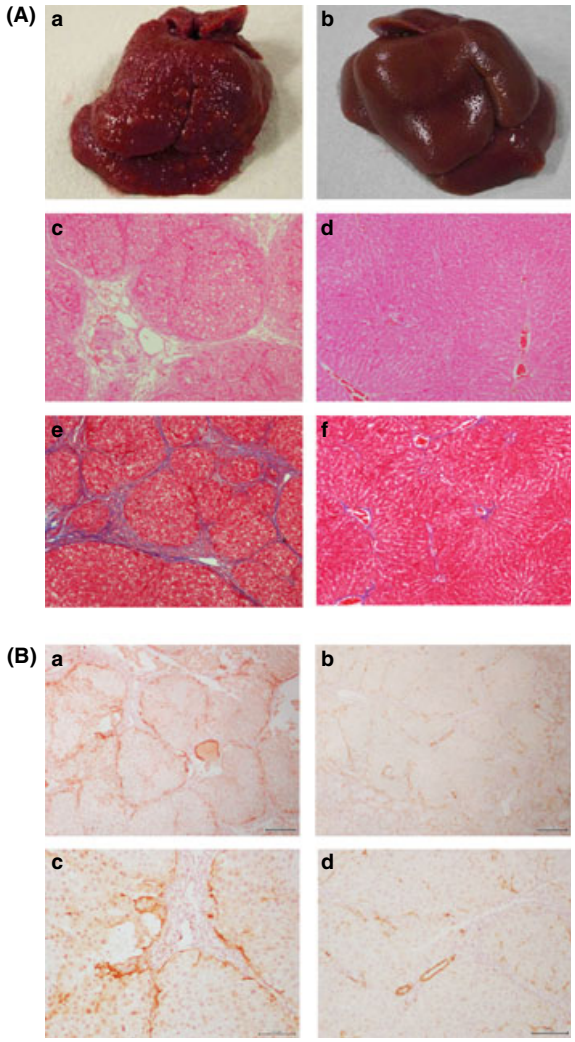

Fig. 6. Effect of CnP on TAA-induced liver fibrosis. (A) Effect of CnP on the morphology of the liver. Rats were treated with TAA for 12 weeks and either vehicle (a, c, e), or 0.9 μg/g CnP (b, d, f) was administered daily. Macroscopic morphology (a, b), HE staining (c, d) and Masson's trichrome staining (e, f) are presented. (B) Effect of CnP on αSMA-positive Cells. Liver specimens obtained from TAA-injected rats treated with vehicle or 0.9 μg/g CnP were immunostained with anti-αSMA antibody. a: vehicle, b: 0.9 μg/g CnP. c, d are higher magnification of a, b respectively.

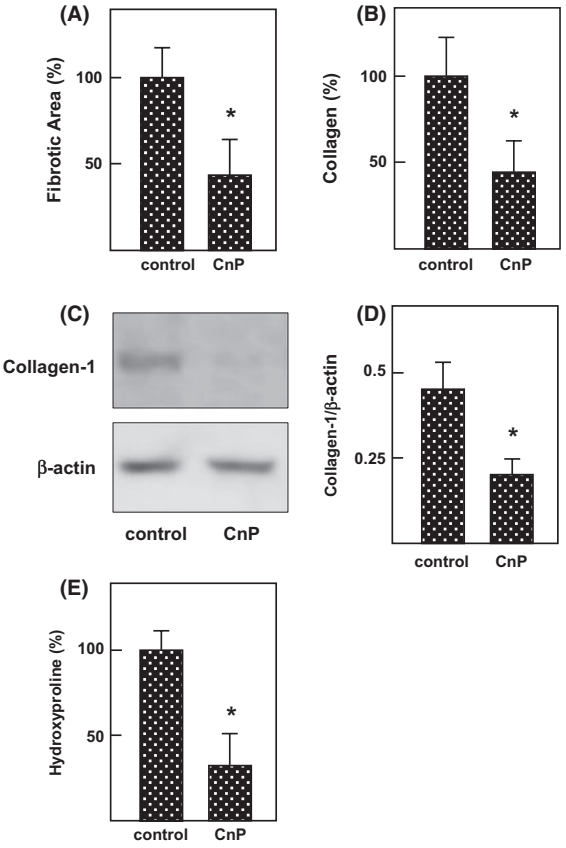

Fig. 7. Effects of CnP on fibrosis and the expression of collagen. (A) Effect of CnP on the fibrotic area. Slices obtained from TAA-injected rats treated with vehicle (control) or 0.9 μg/g CnP were stained with Masson's trichrome and fibrotic area was measured. Values are the mean ± SD (n = 9). *P < 0.05 vs control. (B) Effect of CnP on the collagen content. Liver extracts were obtained from TAA-injected rats treated with vehicle (control) or 0.9 μg/g CnP and the collagen content was measured. Values are the mean ± SD (n = 9). *P < 0.05 vs control. (C) Effect of CnP on the expression of collagen 1. Expression of the collagen-1 was measured by immunoblotting. (D) Quantification of the expression of collagen-1. Results obtained in (C) were quantified by densitometry. Values are the mean ± SD (n = 9). *P < 0.05 vs without CnP. (E) Effect of CnP on the hydroxyproline content. Liver extracts were obtained from TAA-injected rats treated with vehicle (control) or 0.9 μg/g CnP and the hydroxyproline content was measured. Values are the mean ± SD (n = 9). *P < 0.05 vs control.

changes typical of cirrhosis induced by TAA were nearly completely blocked by CnP. Unfortunately, CnP was less effective on established liver fibrosis induced by TAA. This may be because of the inability of CnP on fibrinolytic processes. CnP is effective in preventing the formation of liver fibrosis.

In conclusion, CnP attenuated activation of HSC *in vitro*. In particular, CnP induced apoptosis of HSC and reduced the production of matrix proteins. *In vivo*, TAA-induced cirrhosis was effectively blocked by simultaneous administration of CnP. Hence, CnP is a potential therapeutic agent to prevent cirrhosis.

Acknowledgements

The authors are grateful to Mayumi Odagiri for her secretarial assistance.

Conflicts of interest: The authors do not have any disclosures to report.

References

1. Geerts A. History, heterogeneity, developmental biology, and function of quiescent hepatic stellate cells. *Semin Liver Dis* 2001; **21**: 311–35.
2. Friedman SL. Mechanisms of hepatic fibrogenesis. *Gastroenterology* 2008; **134**: 1655–69.
3. Friedman SL. Molecular regulation of hepatic fibrosis, an integrated cellular response to tissue injury. *J Biol Chem* 2000; **275**: 2247–50.
4. Torok NJ. Recent advances in the pathogenesis and diagnosis of liver fibrosis. *J Gastroenterol* 2008; **43**: 315–21.
5. Tacke F, Luedde T, Trautwein C. Inflammatory pathways in liver homeostasis and liver injury. *Clin Rev Allergy Immunol* 2009; **36**: 4–12.
6. Brenner DA, Waterboer T, Chi SK, *et al.* New aspects of hepatic fibrosis. *J Hepatol* 2000; **32**: 32–8.
7. Taimr P, Higuchi H, Kocova E, *et al.* Activated stellate cells express the TRAIL receptor-2/death receptor-5 and undergo TRAIL-mediated apoptosis. *Hepatology* 2003; **37**: 87–95.
8. Modol T, Natal C, Perez de Obanos MP, *et al.* Apoptosis of hepatic stellate cells mediated by specific protein nitration. *Biochem Pharmacol* 2011; **81**: 451–8.
9. Umezawa K, Ohse T, Yamomoto T, Koyano T, Takahashi Y. Isolation of a new vinka alkaloid from the leaves of *Ervatamia microphylla* as an inhibitor of ras functions. *Anticancer Res* 1994; **14**: 2413–8.
10. Umezawa K, Hiroki A, Kawakami M, *et al.* Induction of insulin production in rat pancreatic acinar carcinoma cells by conophylline. *Biomed Pharmacother* 2003; **57**: 341–50.
11. Mashima H, Ohnishi H, Wakabayashi K, *et al.* Betacellulin and activin A coordinately convert amylase-secreting pancreatic AR42J cells into insulin-secreting cells. *J Clin Invest* 1996; **97**: 1647–54.
12. Ogata T, Li L, Yamada S, *et al.* Promotion of β-cells differentiation by conophylline in fetal and neonatal rat pancreas. *Diabetes* 2004; **53**: 2596–602.
13. Ohnishi N, Miyata T, Ohnishi H, *et al.* Activin A is an autocrine activator of rat pancreatic stellate cells: potential therapeutic role of follistatin for pancreatic fibrosis. *Gut* 2003; **52**: 1487–93.
14. Saito R, Yamada S, Yamamoto Y, *et al.* Conophylline suppresses pancreatic stellate cells and improves islet fibrosis in Goto-Kakizaki rats. *Endocrinology* 2012; **153**: 621–30.
15. Fujii M, Takei I, Umezawa K. Antidiabetic effect of orally administered conophylline-containing plant extract on streptozotocin-treated and Goto-Kakizaki rats. *Biomed Pharmacother* 2009; **63**: 710–6.
16. Weiskirchen R, Gressner AM. Isolation and culture of hepatic stellate cells. *Methods Mol Med* 2005; **117**: 99–113.
17. Xu L, Hui AY, Albanis E, *et al.* Human hepatic stellate cell lines, Lx-1 and Lx-2: new tools for analysis of hepatic fibrosis. *Gut* 2005; **54**: 142–51.
18. Yasuda H, Mine T, Shibata H, *et al.* Activin A: an autocrine inhibitor of initiation of DNA synthesis in rat hepatocytes. *J Clin Invest* 1993; **92**: 1491–6.
19. Ogata T, Li L, Seno M, Kojima I. Reversal of streptozotocin-induced diabetes by transplantation of β-cells derived from ductal cells. *Endocr J* 2004; **51**: 381–6.
20. Reddy GK, Enwemeka CS. A simplified method for the analysis of hydroxyproline in biological tissues. *Clin Biochem* 1996; **29**: 225–9.
21. Nagai T, Miyawaki A. A high-throughput method for development of FRET-based indicators for proteolysis. *Biochem Biophys Res Commun* 2004; **319**: 72–7.
22. Nagasawa M, Kojima I. Translocation of calcium-permeable TRPV2 channel to the podosome: its role in the regulation of podosome assembly. *Cell Calcium* 2012; **51**: 186–93.
23. Sobrevals L, Rodriguez C, Romero-Trevejo JL, *et al.* Insulin-like growth factor I gene transfer to cirrhotic liver induces fibrolysis and reduces fibrogenesis leading to cirrhosis reversion in rats. *Hepatology* 2010; **51**: 912–21.
24. Maher JJ. Interactions between hepatic stellate cells and the immune system. *Semin Liver Dis* 2001; **21**: 417–26.
25. Hinz B, Phan SH, Thannickal VJ, *et al.* The myofibroblast: one function, multiple origins. *Am J Pathol* 2007; **170**: 1807–16.
26. Friedman SL. Hepatic stellate cells. *Prog Liver Dis* 1996; **14**: 101–30.
27. Maher JJ, McGuire RF. Extracellular matrix gene expression increases preferentially in rat lipocytes and sinusoidal endothelial cells during hepatic fibrosis in vivo. *J Clin Invest* 1990; **86**: 1641–8.
28. Kojima I, Umezawa K. Conophylline: a novel differentiation inducer for pancreatic β cells. *Int J Biochem Cell Biol* 2006; **38**: 923–30.
29. Weng TC, Shen CC, Chiu YT, Lin YL, Huang YT. Effects of amepavine against hepatic fibrosis induced by thioacetamide in rats. *Phytother Res* 2012; **26**: 344–53.
30. Patella S, Phillips DJ, Tchongue J, de Kretser DM, Sievert W. Follistatin attenuates early liver fibrosis: effects on hepatic stellate cell activation and hepatocyte apoptosis. *Am J Physiol Gastrointest Liver Physiol* 2006; **290**: G137–44.
31. Tsai MK, Lin YL, Huang YT. Effects of salvianolic acids on oxidative stress and hepatic fibrosis in rats. *Toxicol Appl Pharmacol* 2010; **242**: 155–64.
32. Wang X, Ikejima K, Kon K, *et al.* Ursolic acid ameliorates hepatic fibrosis in the rat by specific induction of apoptosis in hepatic stellate cells. *J Hepatol* 2011; **55**: 379–87.
33. Arthur MJ. Reversibility of liver fibrosis and cirrhosis following treatment for hepatitis C. *Gastroenterology* 2002; **122**: 1525–8.
34. Iredale JP. Hepatic stellate cell behavior during resolution of liver injury. *Semin Liver Dis* 2001; **21**: 427–36.
35. Wright MC, Issa R, Smart DE, *et al.* Gliotoxin stimulates the apoptosis of human and rat hepatic stellate cells and enhances the resolution of liver fibrosis in rats. *Gastroenterology* 2001; **121**: 685–98.

36. Elsharkawy AM, Oakley F, Mann DA. The role and regulation of hepatic stellate cell apoptosis in reversal of liver fibrosis. *Apoptosis* 2005; **10**: 927–39.

37. Shu JC, He YJ, Lv X, Ye GR, Wang LX. Curcumin prevents liver fibrosis by inducing apoptosis and suppressing activation of hepatic stellate cells. *J Nat Med* 2009; **63**: 415–20.